Design and characterization of an integrated Remote Access Unit for wireless communication

K. Rylander*, S. Latkowski†, G. Dabos‡, M. Moralis-Pegios‡, E. Bente†,
R. Broeke§, D. Tsiokos‡, N. Pleros‡, A. Sosa‖, T. Tekin‖ and A. Bakker*
*PhoeniX Software, Hengelosestraat 705, 7521 PA Enschede, Netherlands
Email: katrin.rylander@phoenixbv.com
†COBRA Research Institute, Eindhoven University of Technology, Den Dolech 2, 5612AZ Eindhoven, Netherlands
‡Department of Informatics, Aristotle University of Thessaloniki, P.O. Box 114, 54124 Thessaloniki, Greece
§Bright Photonics, Burgemeester van den Helmlaan 67, 3604 CE Maarssen, Netherlands
‖Research Center of Microperipheric Technologies,Technische Universitaet Berlin,
Gustav-Meyer-Allee 25, 13355 Berlin, Germany

***Abstract*—We present the design and experimental evaluation of a Remote Access Unit (RAU) that integrates Radio-Over-Fiber (RoF) with 60 GHz wireless (10-20 GHz on-chip) and Fiber to the Home (FTTH) services. The Indium Phosphide chip was manufactured within Multi Project Wafer run and characterized in terms of DC and high speed transmission.**

Keywords - Photonic Integrated Circuit, Multi Project Wafer Run, Fiber To The Home, Radio over Fiber

I. Introduction

Mobile data usage is projected to grow three times faster than IP traffic from fixed lines, while operators of wireless networks are already reaching the throughput limits of existing technologies [1]. One way to overcome this problem, as proposed by the COMANDER project [2], is to merge currently distinct optical and wireless infrastructures. Presented solution builds upon the Radio-over-Fiber paradigm and provides a large flexibility since it can coexist with all the already deployed optical systems. The key component of such Next Generation Network [3] is a Remote Access Unit (RAU), capable of simultaneously supporting end users with mobile and broadband Fiber-To-The-Home (FTTH) services. Here we report on the design and development of RAU and measured performance of its all subsystems.

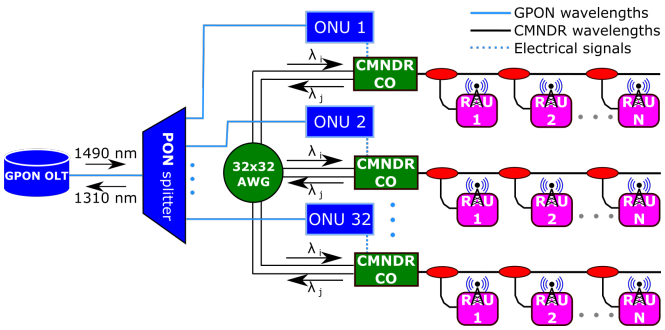

Fig. 1. COMANDER Network in GPON.

II. Chip design and fabrication

RAU, shown schematically in Fig. 2, was designed as a photonic integrated circuit (PIC) on an Indium Phosphide platform following the generic integration concept [4]. The advantage of PIC technology compared to bulk optics is more compact and mechanically stable devices. Miniaturization potentially leads to a lower power consumption, making the final products more energy efficient [5], [6]. Moreover, high level of integration and shorter interconnects increase the reliability of the devices in terms of phase stability. The use of a Multi Project Wafer (MPW) runs simplifies the prototyping stages and allows low-cost access to the technology, as fabrication costs are shared between users.

The layout of RAU has been designed in OptoDesigner5, using foundry provided Photonic Design Kit (PDK) and an AWG IP Block. The chip was fabricated by Oclaro and HHI foundries [4] in MPW runs accessed via PARADIGM project [7]. Since porting designs between foundries is supported by the software tools [8] it took 3 designers only 1 month to successfully complete 2 foundry specific layouts of the RAU chip. The work reported here concerns design and characterization of PIC based on HHI-PDK.

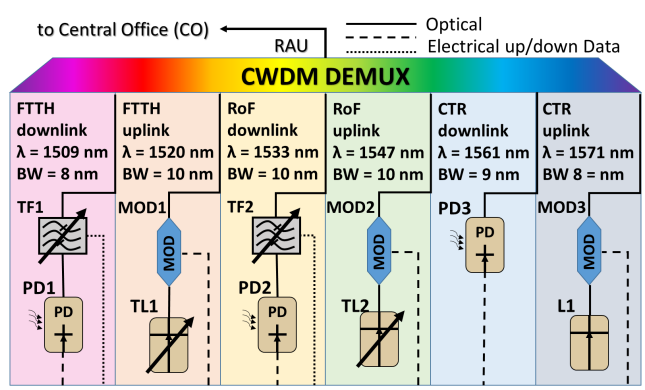

Fig. 2. Schematic diagram of the RAU. CTR = Control signals, TF = Tuneable Filter, PD = Photo Diode, MOD = Modulator, TL = Tuneable Laser.

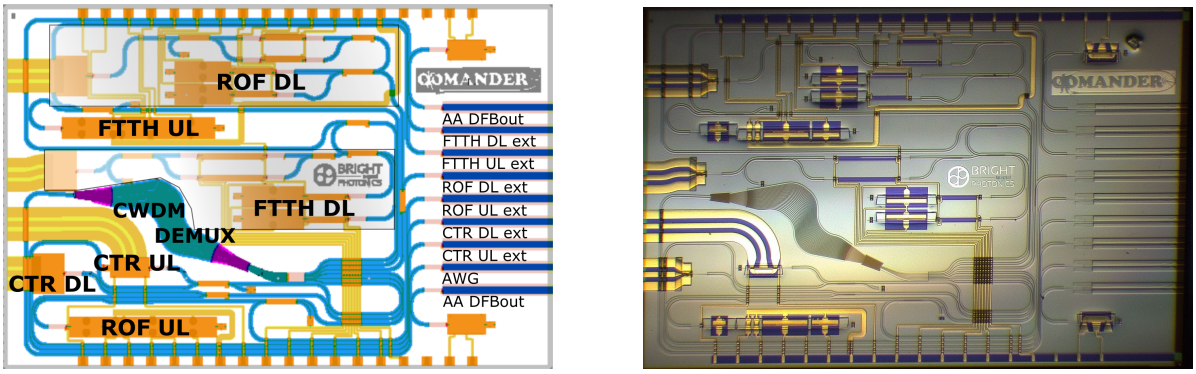

(a) (b)

Fig. 3. (a) Mask layout of Remote Access Unit. (b) Fabricated photonic chip. The size of a chip is 4 mm × 6 mm.

Designed RAU utilizes a Coarse Wavelength Division Multiplexing (CWDM) demultiplexer (DEMUX) to provide six discrete spectral passbands. In full operation all signals are processed simultaneously by specifically designed sub-circuits. Therefore, in order for the RAU to be operational, the central wavelengths of transmitters and receivers (Fig. 2) have to match the channels of demultiplexer. Fig. 3 shows the mask layout submitted to the foundry along with the photograph of the fabricated chip.

III. Experimental setups

The chip was mounted on an aluminum sub-carrier and electrical contacts were wire - bonded to DC tracks on a printed circuit board providing with several feed lines. Since all Radio Frequency (RF) contacts were accessible on one side of the chip, a Ground-Signal-Ground RF probe was used for driving. The chip temperature was stabilized at 19°C by water cooling of the metal sub-carrier in case of DC and by Peltier element for high speed measurements. A comercially available fiber array unit of single mode fibers was used to couple the signals into and from the chip. Fig. 4 show the schematics of experimental setups used.

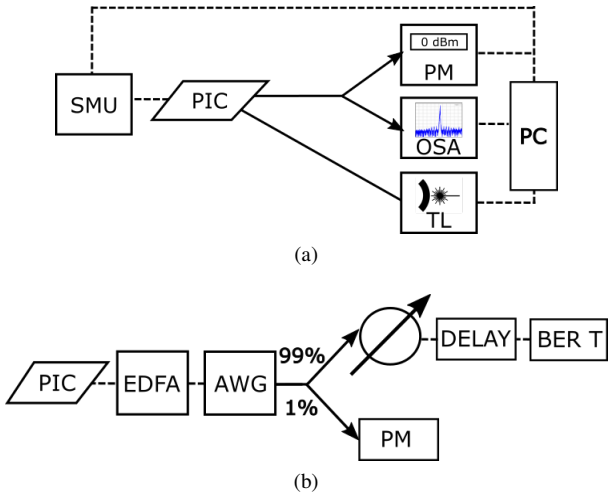

Fig. 4. (a) Experimental setup for DC characterization: Source Meter Unit (SMU), Power Meter (PM), Optical Spectrum Analyzer (OSA), Tunable Laser (TL), Computer (PC) with dedicated software for measurement automation. (b) Experimental setup for Bit Error Rate (BER) measurement: Erbium Doped Fiber Amplifier (EDFA), AWG filter, 99/1 power splitter, optical delay line (DELAY), BER tester (BER T)

IV. Results

A. Multiplexer/Demultiplexer

CWDM DEMUX was realized as an Arrayed Waveguide Grating (AWG) with a central wavelength of 1540 nm, a free spectral range of 100 nm, flattened passbands and a non-constant channel spacing. Fig. 5 shows the comparison between the measured spectral response of the AWG (TE polarization) and corresponding simulation data. Results were normalized in order to eliminate the influence of different coupling conditions between the AWG channels as well as to compensate for a central wavelength shift. Afer normalization, the noise levels of all measured passbands reached the same value which supports the validity of the used method. An offset of +7.2 nm in central wavelength of AWG, which stems

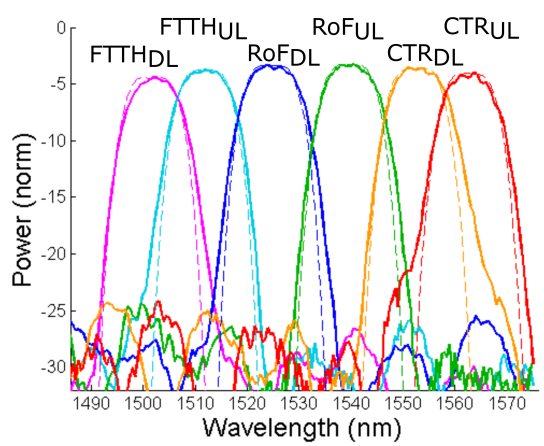

Fig. 5. Measured (solid line) versus simulated (dashed line) spectral responses of the AWG for TE polarization. The maximum power per channel was normalized to match the peak values obtained from the simulations.

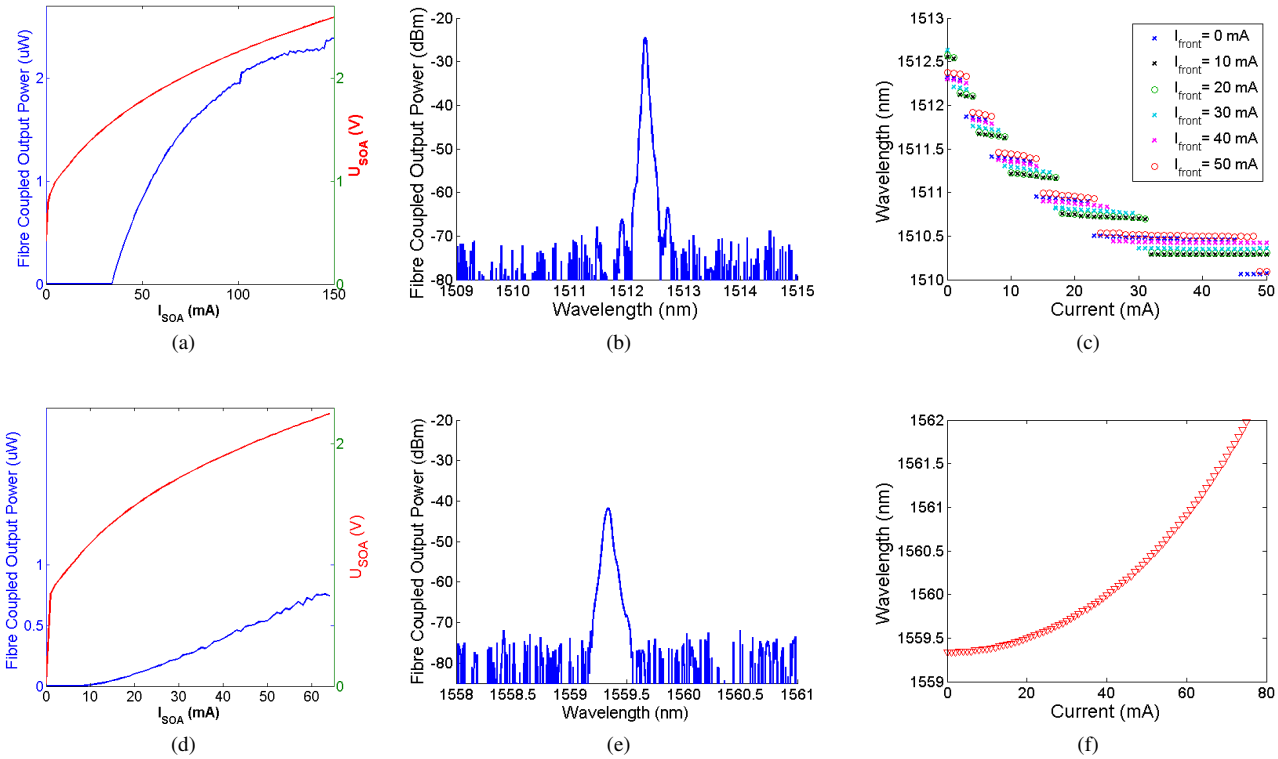

Fig. 6. (a) Optical power and voltage across the gain section against injected current. (b) Emission spectrum for gain section bias = 150 mA and booster bias = 40 mA, Full Width at Half Maximum (FWHM) = 0.05 nm. (c) Wavelength tuning with front and rear grating bias. (d) Optical power and voltage across the gain section against injected current. (e) Emission spectrum for gain section bias = 18 mA, FWHM = 0.05 nm. (f) Wavelength tuning with heater bias.

from process tolerances, was reported in the previous HHI MPW run. Therefore, the central wavelength of AWG was calibrated by this value during the design stage. However, in this run the wavelength offset was of about -0.5 nm, leading to a 7.7 nm blue shift in central wavelength of the fabricated AWG. Normalized data show a satisfactory overlap between designed and obtained filter response when it comes to channels distribution and the 3-dB bandwidths (BW). Measured cross-talk is about 20 dB and typical for HHI platform [9], while measured offset between central wavelengths for TE and TM response is equal 1.2 nm.

B. Tuneable Transmitters: DC response

The chip contains three transmitters: two tuneable Distributed Bragg Reflector (DBR) lasers inside FTTH UL and RoF UL transmitters and a Distributed Feedback (DFB) laser in the control uplink (CTR UL) sub-circuit. The lasers were designed for central wavelengths of 1522 nm, 1549 nm and 1570 nm, respectively. Voltage measured across the gain sections and fiber coupled output power against the injected current characteristics along with wavelength tuning curves for FTTH and CTR lasers are presented in Fig. 6.

Measured threshold current is about 35 mA for the FTTH and about 8 mA for the CTR laser, which matches HHI specification. However, due to some fabrication issues in the definition of Bragg gratings, all lasers exhibit a blue shift in the central wavelength of nearly 10 nm with respect to the specified values. This offset in central wavelength matches well the AWG response shift and allows operability of all transmitters. The drawback of gratings imperfections is the multi-mode behaviour of the DFB laser. Moreover, high losses of transition building blocks result in 14 dB lower than expected output power of all lasers. The side mode suppression ratio (SMSR) of the FTTH laser varies with the gain section bias from 25 to 45 dB. It can be noted from Fig. 6c that the maximum possible blue shift of the central wavelength, obtained by biasing front and rear gratings, is 2.57 nm. The free spectral range (FSR) is equal 0.4 nm and corresponds well to the cavity length of 770 μm. The SMSR of the CTR laser varies with the gain section bias from 10 to 33 dB. From Fig. 6f it can be observed that the maximum possible red shift of the central wavelength, obtained by biasing the built-in heater, is 2.75 nm. The FSR equals 4 nm which corresponds to the cavity length of 82 μm.

C. Tuneable Transmitters: RF response

High speed response was investigated for RoF UL and CTR UL lasers. Due to their low output power it was necessary to use an external, erbium doped fiber amplifier - EDFA (see Fig. 4b). The central wavelength of FTTH UL transmitter lies outside of the operating wavelength range of available EDFAs therefore it was not possible to characterize its high speed performance.

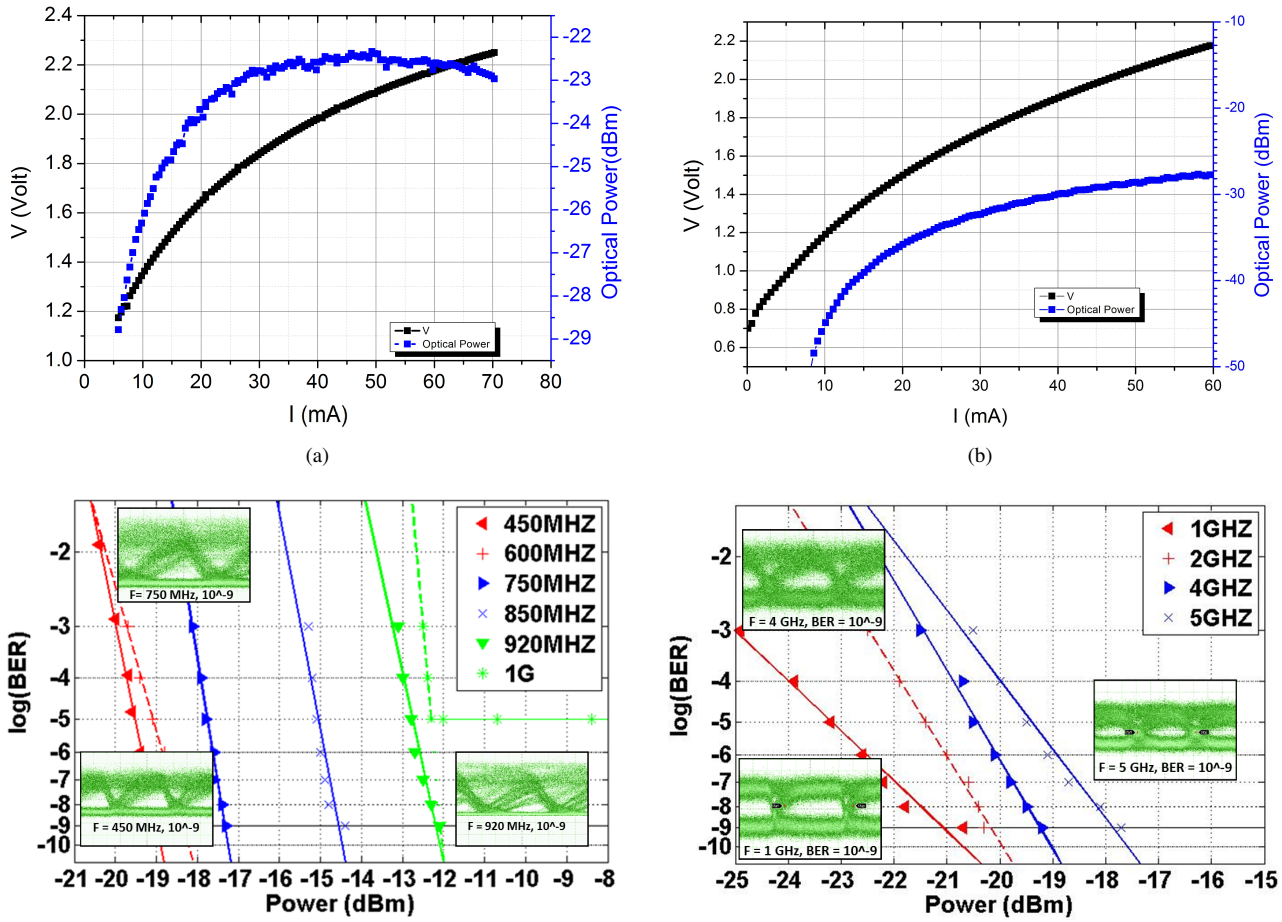

Fig. 7. (a) Power-Current-Voltage (PIV) curve for RoF UL transmitter (current and voltage were measured across the SOA switch). (b) PIV curve for CTR UL transmitter. (c) BER curve for RoF UL transmitter. (d) BER curve for CTR UL transmitter.

In the first stage a power-current-voltage test was performed for both transmitters to estimate their on/off optical extinction ratio (ER) and operating point. CTR UL laser was directly modulated while for RoF UL a short SOA (Semiconductor Optical Amplifier) switch in front of the DBR laser was used instead. As presented in Fig. 7a, 7b ER for the RoF UL transmitter equals 6 dB and 20 dB for the CTR UL. As a next step the spectral responses for 'on' and 'off' states were compared for each transmitter. Results indicate that the central wavelength increases and SMSR decreases in 'on' state as the side modes gain more power. In order to supress these effects, an AWG was added behind EDFA to filter out the unwanted longitudinal modes. The bit error tate (BER) was measured by transmitting a known pseudo-random binary sequence and comparing it with the received signal. The optical power before the receiver was varied with optical attenuator and corresponding BER was recorded. In these measurements, the decision threshold was optimized for each transmitter speed [10]. All measurements were performed in back-to-back configuration, formed by connecting the transmitter directly to the receiver. Eye diagrams obtained for RoF UL exhibit high noise level (Fig. 7c) originating mainly from SOA intrinsic noise. Another noise source can stem from the lack of impedance matched RF connection and using a DC wire instead. Presence of multiple levels that correspond to logic one significantly limits modulation speed to about 1 GHz. BER curve obtained for 1 GHz shows the noise floor of 10^{-5}.

CTR UL transmitter, which was biased with a Ground-Signal-Ground RF probe connected to an impedance matched metal track exhibits much better high speed performance and offers modulation speeds up to 5 GHz.

D. Tuneable Receivers

Tuneable filters for FTTH DL and RoF DL receivers were designed as a cascade of asymmetric Mach-Zehnder and Michelson interferometers. Bragg gratings were added into both arms of the Michelson interferometer as reflective elements [11]. Measured spectral response shows that the filter offers 3-dB BW of 0.6 nm and the ER of 4.6 dB. The filter is more selective than required 3-dB BW of 1 nm, however the extinction ratio is lower than calculated by nearly 5 dB. Fig. 8 shows measurement data obtained for different phase shifts, introduced by Michelson Interferometer with FSR of

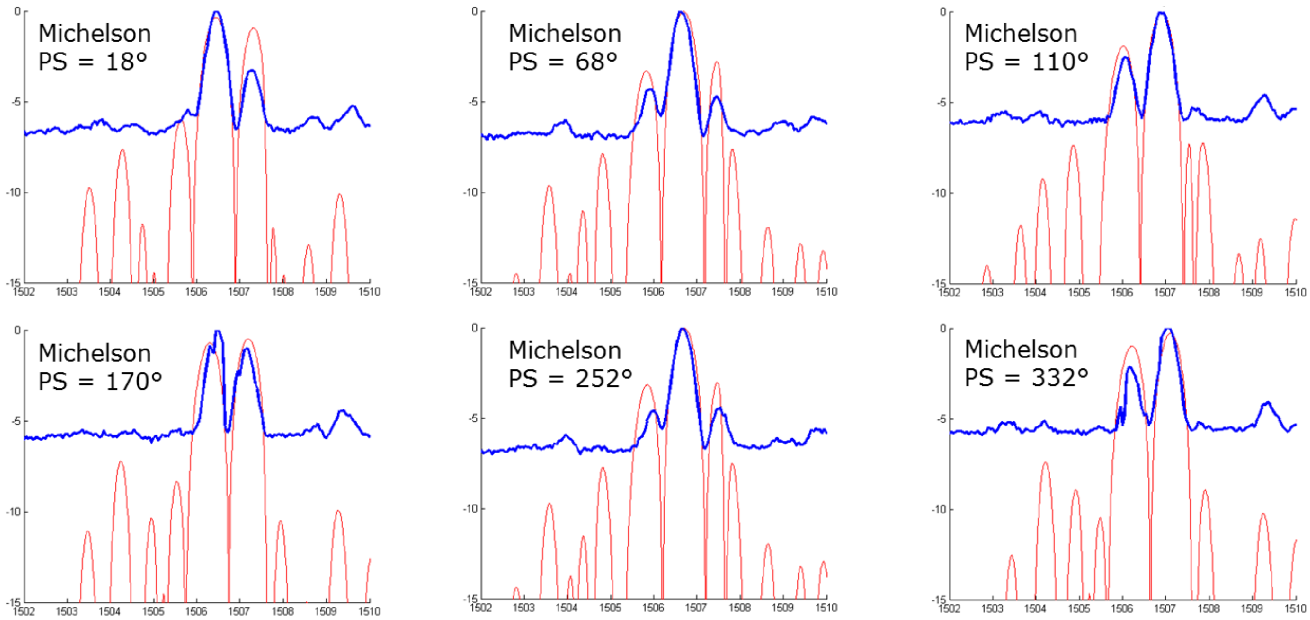

Fig. 8. Filter response for various phase shifts (PS) introduced by Michelson Interferometer.

1 nm, and overlaid with the simulation results. High noise level of the measured data, originating from high coupling losses of over 10 dB and AWG insertion losses does not allow to make a more detailed comparison.

Conclusions

DC characterization results show that majority of the subsystems on fabricated RAU is operational. RF characterization results indicate that using a SOA section in front of a DBR laser for on-off keying cannot provide modulation speeds higher than 1 GHz. On the contrary, DFB lasers on HHI platform have a potential to provide modulation speeds of several GHz, which is sufficient for the COMANDER network. Finally, the new concept of a tunable filter based on a cascade of Michelson and MZI interferometers was proved to work.

Acknowledgments

The research leading to these results has received funding from EU FP7-PEOPLE-2013-IAPP under grant agreement 612257 COMANDER and EU FP7/2007-2013 under grant agreement ICT 257210 PARADIGM.

References

[1] http://www.ftthcouncil.eu/documents/Publications/DandO_White_Paper_2013_Final.pdf
[2] http://mc-comander.eu/
[3] C. Ranaweera, E. Wong, C. Lim and A. Nirmalathas, 'Next generation optical-wireless converged network architectures,' IEEE Network, vol.26, Iss.2, pp. 22 27, 2012.
[4] M. Smit et al., 'An introduction to InP-based generic integration technology,' Semiconductor Science and Technology, vol. 29, Iss. 8, 2014.
[5] Q. Cheng, A. Wonfor, R.V. Penty, I.H.White, 'Scalable, low-energy hybrid photonic space switch,' J. Lightwave Technology, vol. 31, Iss. 18, pp. 307784, 2013.
[6] R. Stabile, A. Albores-Mejia, A. Rohit, K. A. Williams, Integrated optical switch matrices for packet data networks, Microsystems & Nanoengineering, vol. 2, article number: 15042, 2016.
[7] http://www.paradigm.jeppix.eu
[8] A. Sosa, K. Welikow, R. Broeke, A. Bakker, D. Tsiokos, T. Tekin, and N. Pleros, 'Demonstrating efficient design transfer methods for complex photonic integrated circuits,' Proceedings of the 19th Annual Symposium of the IEEE Photonics Benelux Chapter, pp. 95-98, 2014.
[9] M. Baier et al.,'100-Channel WDM Rx-Type PIC on InP for Use of Low-Cost and Low Power Consumption Electronics,' The European Conference on Optical Communication (ECOC), 2014
[10] A. Stavdas, 'Core and Metro Networks,' Wiley, ch.3, pp.149-158, 2010, ISBN-13: 9780470512746
[11] K. Rylander, R. Broeke, R. Stoffer, D. Melati, A. Melloni, A. Bakker,'Design of integrated, tuneable filters for telecom application,' Proceedings of the 18th European Conference on Integrated Optics, 2016.